The Angular Dependence of Compton Scattering Cross-section Ratios of Cu and Al

Alin Airinei*
Department of Physics, Stony Brook University, Stony Brook, NY 11794
(Dated: May 2020)

To determine the angle dependence of the energy shift of scasttered photons from low and high density metals such as Al and Cu,monoenergetic gamma rays sourced from Cs-137 were used in conjunction with a NaI scintillator-photomultiplier detector.

I. Introduction

I.1. Theory

In the original (1923) paper on the quantum theory of light scattering [1], A.H. Compton chalenged the classical Thomson model of wave-matter interaction on the premise that the observed shift in wavelength due to scattering of energetic X-rays or gamma rays from weakly bound electrons can more appropriately be described by a particle-like interaction between the incident "radiation quantum" and the electron, with the result that after recoil a sufficient frequency shift will occur to produce a lower energy photon with the difference in energy being transfered to the electron.

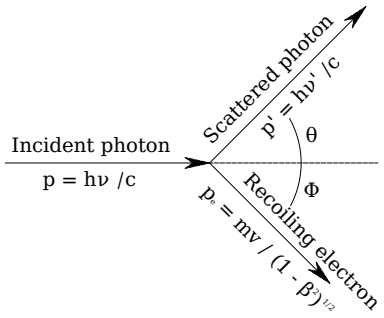

Figure 1. Digram showing the scattering process with the incident photon being scattered from an electron initially at rest.

As shown in Fig. 1 the Compton scattering mechanism consists of a photon of initial momentum $h\nu_0/c$ scattering from an electron of mass m at an angle θ with the initial momentum and a final momentum of the scattered ray equal to $h\nu_\theta/c$.

Therefore, based on the conservation principle, the momentum of recoil of the scattering electron is given by the vector difference of the incident and scattered ray as[1]:

$$\left(\frac{m\beta c}{\sqrt{1-\beta^2}}\right)^2 = \left(\tfrac{h\nu_0}{c}\right)^2 + \left(\tfrac{h\nu_\theta}{c}\right)^2 + 2\tfrac{h\nu_0}{c}\cdot\tfrac{h\nu_\theta}{c}cos\theta \quad (1)$$

where $\beta = v_e/c$. We, also know that the final energy of the scattered ray will be equal to the initial energy minus the kinetic energy which was transfered to the electron:

$$h\nu_\theta = h\nu_0 - mc^2\left(\frac{1}{\sqrt{1-\beta^2}} - 1\right) \quad (2)$$

Solving Eqn. (2) for β we obtain an expression which gives us the velocity of the electron after recoil as a function of the frequency of the incoming and scattered rays and, implicitly, as a function of the scattering angle:

$$\beta = \sqrt{\frac{2h^2\nu_\theta\nu_0 - 2mc^2h\nu_\theta - 2mc^2h\nu_0 + h^2\nu_\theta^2 + h^2\nu_0^2}{m^2c^4 - 2mc^2h\nu_\theta - 2mc^2h\nu_0 + 2h^2\nu_\theta\nu_0 + h^2\nu_\theta^2 + h^2\nu_0^2}} \quad (3)$$

To find the frequency (and implicitly the energy) of the scattered ray we substitute (3) into (1) to obtain:

$$h\nu_\theta = \frac{h\nu_0}{1+\alpha(1-cos\theta)} \quad (4)$$

where $\alpha = h\nu_0/mc^2$. This can be rearranged as:

$$\frac{1}{h\nu_\theta} - \frac{1}{h\nu_0} = \frac{1}{m_e c^2}(1-cos\theta) \quad (5)$$

One of the main goals of this experiment is to prove Eqn. (5).

The differential cross section for Compton scattering as a function of angle is given by the Klein-Nishina equation as:

$$\frac{d\sigma}{d\Omega} = r_0^2\frac{1+cos^2\theta}{2}\frac{1}{[1+\alpha(1-cos\theta)]^2} \times\left[1+\frac{\alpha^2(1-cos\theta)^2}{(1+cos^2\theta)[1+\alpha(1-cos\theta)]}\right] \quad (6)$$

The Klein-Nishina result is an improvement over the classical Thomson cross section which assumes the electron is static and does not account for quantum and relativistic effects[5].

* alin.airinei@stonybrook.edu
zachary.kluger@stonybrook.edu

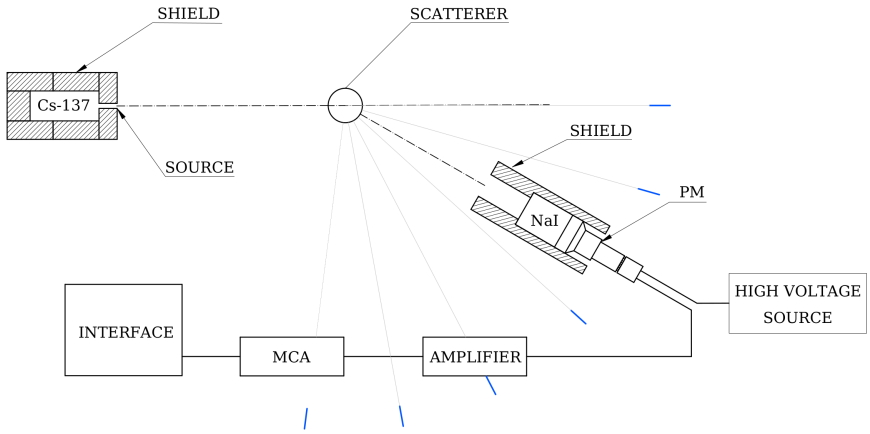

Figure 2. Diagram showing the scattering process with the incident photon being scattered from an electron initially at rest.

I.2. Experimental Setup

A schematic representation of the of the apparatus used in the experiment is shown in Fig. 2. The ^{137}Cs source is enclosed by lead bricks. The target is fixed in place on the rotating platform in front of the detector which can thus "orbit" around it and record different scattering angles.

Enclosed in the detector shield is a sodium iodide scintillation crystal and a photomultiplier tube. The working principle of the scintillation detector is related to the same processes that produce the scattering in the first place i.e. Compton scattering, photoelectric absorption, X-ray production, and pair production with the Compton scattering being the most probable for all the range of $\gamma - ray$ energies [3, 4].

As a $\gamma - ray$ transfers it's energy to a weakly bound electron in the detector (photoelectric effect), will cause a chain reaction in which the electron will give up it's newly acquired kinetic energy by creating ionization and visible light photons. The light produced is proportional with the energy transferred by the incident gamma-ray[4].

The light thus produced is further detected and amplified by a photomultiplier. As the photons enter the multiplier they will eject new electrons which are accelerated through a set of electrodes causing secondary emissions. At the opposite end the electric signal will be proportional to the energy of the original ray [4].
indent Also schematically shown in the diagram are are the multi channel analyzer (MCA) which assigns the measured energies to channels, and the computer interface wich records and controls the measurements using the Maestro software.

II. Results

II.1. Calibration

The spectrum of different weak sources was measured to calibrate the energy scale. For an initial estimate, the .spe files generated by by the Maestro interface were loaded into the InterSpec application which detects the peaks based on detector type and characteristics and it's library of known spectra.

Comparing data collected on different days (possibly taken different by groups) there were observed differences in the spectra. These differences could be explained by a number of factors such as the use of different settings, different source height and distance from the detector, and the use of samples of different strength.

The graph in Fig. 3 shows the ^{137}Cs spectrum with measurements collected on September 12, 2018. The peaks and their relative intensities were detected both by the InterSpec application and cross-referenced with the gamma-ray spectrum catalogue referenced in [6].

The known values for all 5 detected peaks together with those for ^{22}Na and ^{133}Ba were used for the final calibration of the energy scale.

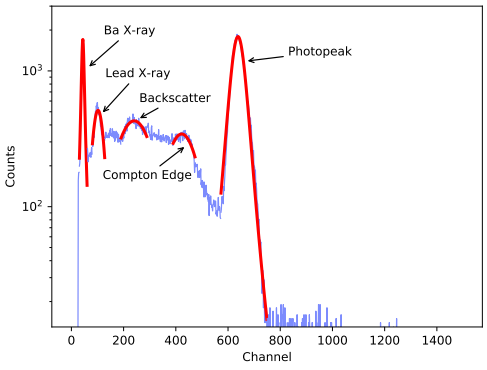

Figure 3. Uncalibrated ^{137}Cs spectrum, showing the leading Ba X-ray peak, the Pb X-ray, backscatter, Compton edge, and the photopeak at 661.657 keV.

In the case of ^{22}Na the highest intensity peak of the spectrum at 511keV does not correspond to a gamma-ray photopeak but is determined by electron-positron annihilation events[6]. The measured spectrum of ^{22}Na is

shown in Fig. 4.

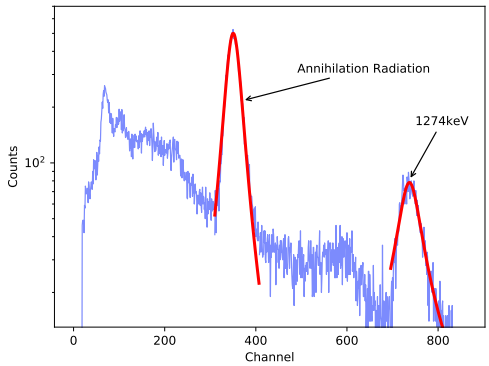

Figure 4. Uncalibrated ^{22}Na spectrum, showing the electron-positron annihilation peak at 511keV and the photopeak at 1274keV.

After taking measurements for ^{137}Cs, ^{22}Na, ^{133}Ba, and ^{57}Co a calibration curve was built. The data was fitted with both a 1st degree polynomial and a second degree polynomial and then the mapping was reversed. In both cases the second degree polynomial yielded better results based on the unweighed χ^2_{red} values for the two models.

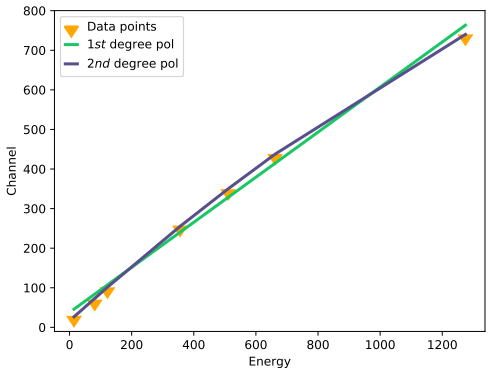

Figure 5. Plot of channel vs energy.

The accuracy of the scintillator is dependent on many factors such as relaxation times, absortpion efficiency, intensity. The uncertainty is usually determined by comparison with high resolution detectors such as HPGe. According to results published in [7] a typical uncertainty for a 3x3 NaI scintillator is about 1.3%. This value was used for an initial estimate of the accuracy of the energy measurements giving for the reversed mapping a $\chi^2_{red} = 1.078$ for the second degree polynomial.

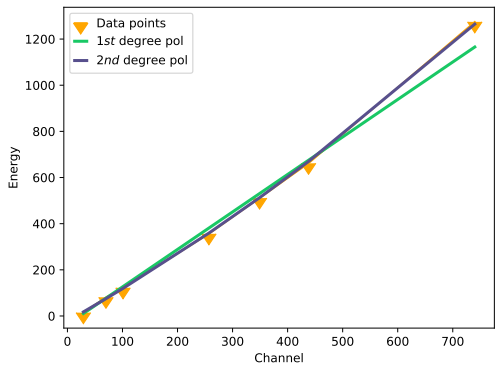

Figure 6. Plot of energy vs channel.

II.2. The scattered photon energy dependence on angle

Using a large aluminum target, the energy of the scattered gamma-ray was measured for a range of angles between 18^o and 110^o . By fitting Compton's formula in the form of Eqn. (5) with $1/E_\theta - 1/E0$ on the y-axis, and $(1 - cos\theta)$ on the x-axis, the resulted slope is expected to be equal to $1/m_e c^2$, and thus the rest mass of the electron can be determined.

From Fig. 6 it can be seen that on the first attempt, the linearity of the results was profoundly affected by the measurements at small angle values where the energy resolution of the incoming and scattered beams is very low, and hence the uncertainty is very high.

The measured value of m_e thus deterimend is $10.696 \times 10^{-31} \pm 9.47 \times 10^{-32}$ Kg, which is in good agreement with the standard value of 9.1094×10^{-31}Kg.

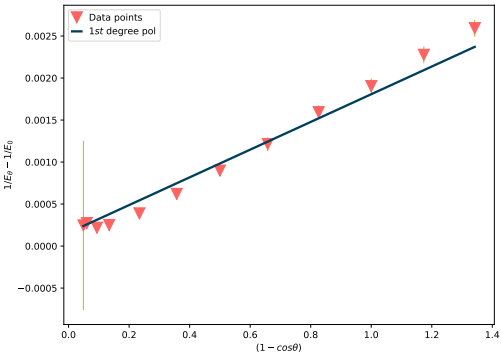

Figure 7. $1/E_\theta - 1/E0$ plottet agains $(1 - cos\theta)$. The non-linearity of the data points is given by the uncertainty in the energy position at the smallest angles.

By removing the values corresponding to the two lowest angles the model yielded a $\chi^2_{red} = 1$ (Fig. 7), and an

electron rest mass equal to $9.5884 \times 10^{-31} \pm 2.28 \times 10^{-32}$.

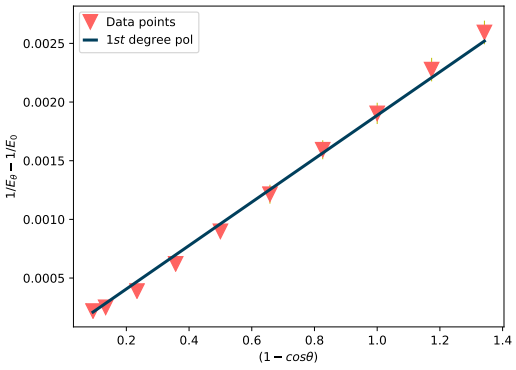

Figure 8. $1/E_\theta - 1/E0$ plottet agains $(1 - cos\theta)$ with the small angle values removed. The fit shows a virtually perfect linear dependence.

III. Conclusions

To optimize the scintillation spectroscopy system used for this experiment, spectra of different weak sources were compared with known values and calibration techniques were applied to align the default channel assignment of the MCA with the corresponding values.

To validate the Compton model of photon scattering from a free electron, a strong ^{137}Cs monoenergetic (661.657keV) was used to measure the angle dependence of the energy of the scattered ray.

We showed that the results are consistent with the particle theory of light by showing that the difference in energy of the scattered and incident ray is proportional with the energy of the electron.

By comparing the results to the Compton model we were able to extract the rest mass of the electron with a good agreement with the accepted value.

[1] A. H. Compton, Physical Review 21, 483 (1923).

[2] The Oskar Klein Memorial Lectures (World Scientific, Singapore, 1994).

[3] J. E. Parks and C. P. Cheney, 2015 Conference on Laboratory Instruction Beyond the First Year (2015).

[4] J.E.Parks. *The Compton Effect - Compton Scattering and Gamma Ray Spectroscopy*.2015. Unpublished, available online at: `http://www.phys.utk.edu/labs/modphys/Compton%20Scattering%20Experiment.pdf`.

[5] A. C. Melissinos and J. Napolitano, Experiments in Modern Physics (Academic Press, Amsterdam, 2015).

[6] Heath, R. L. Scintillation Spectrometry: Gamma-Ray Spectrum Catalogue. U.S. Atomic Energy Commission, Idaho Operations Office, 1964.

[7] Bu, Minqiang, et al. Characterisation of Scintillator-Based Gamma Spectrometers for Determination of Sample Dose Rate in OSL Dating Applications. Radiation Measurements, vol. 120, 2018, pp. 253259., doi:10.1016/j.radmeas.2018.07.003.

PHY445_Lab3_Compton

May 23, 2020

[1]:
```
#Part1: Using the jupyter-notebook

import numpy as np
import matplotlib.pyplot as plt

#generating
mu, sigma = 0, 0.1 #mean and stdev
s = np.random.normal(mu, sigma, 1000)

count, bins, ignored = plt.hist(s, 1000, density=True)
plt.plot(bins, 1/(sigma * np.sqrt(2 * np.pi)) * np.exp( - (bins - mu)**2 / (2 *␣
 ↪sigma**2) ), linewidth=2, color='r')


plt.show()
```

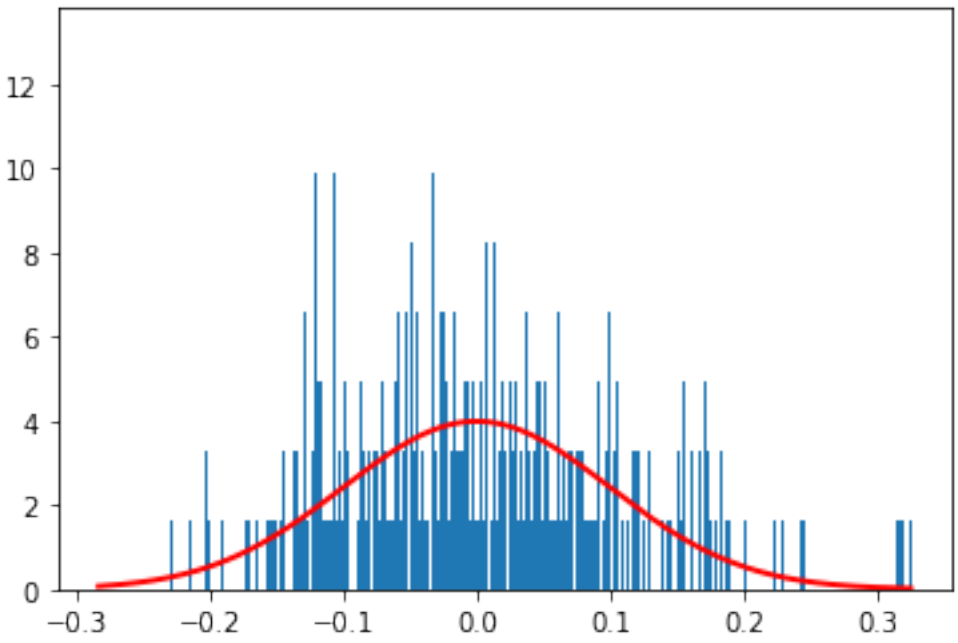

[18]:
```
import numpy as np
from numpy import sqrt, pi, exp, linspace, loadtxt
from lmfit.models import GaussianModel, PolynomialModel
import matplotlib.pyplot as plt

data = loadtxt('180912_1554_Calib_Cs-137.csv')
s = data[:]

bins=np.linspace(0, 1, 2047)

plt.hist(s, 750, density=True)

plt.xlim(-10, 750)
plt.yscale('log')

plt.show()
```

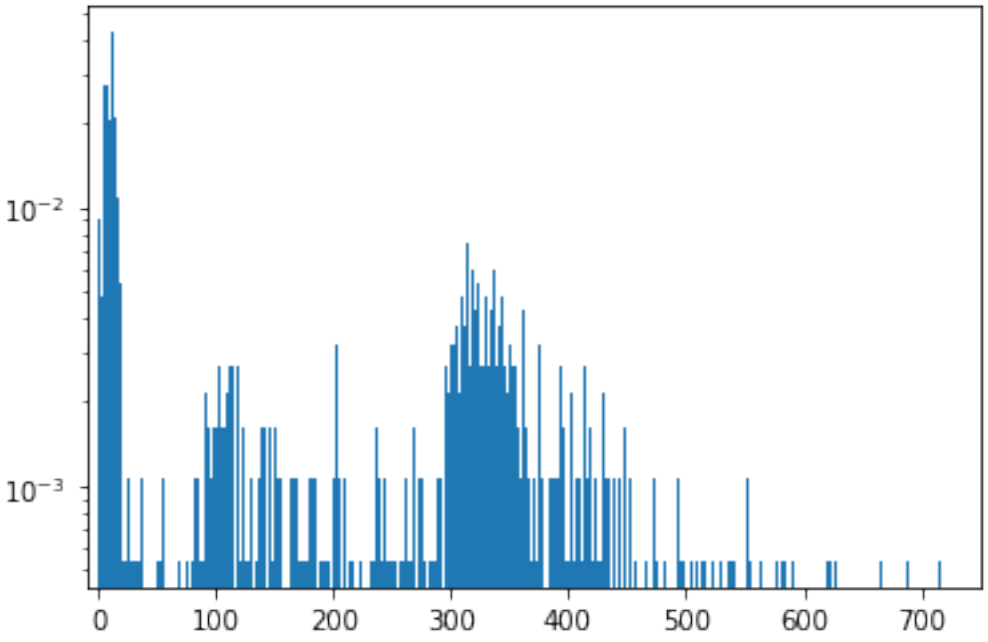

[ ]: